

INTRODUCTION

How does the sun affect us and why do we care?

The Sun is arguably the most relevant astrophysical object to humanity. Its distance from the earth defines a Goldilocks zone (not too hot, not too cold) in which human life can exist. Most of the energy that we use daily can be attributed to the sun, from the obvious solar power, to wind and hydro power (driven by weather created by the sun), to fossil fuels formed from the decay of organic organisms of the past. The rising and setting of the sun defines the daily human experience. Despite our reliance on the sun it is often underappreciated by us and overlooked by physicists who choose to study supposedly more ‘sexy’ astrophysical objects much further away.

In addition to being essential to life on earth, the sun is very violent and energetic. The sun is constantly blasting the earth with radiation and high energy particles. Luckily the earth’s atmosphere and magnetic field protects us from both. The earth’s atmosphere absorbs a large portion of the solar radiation, some of which (x-ray and ultraviolet) can be quite harmful to humans. The earth’s magnetic field steers most energetic particles around earth. Despite these protections we are not immune to the sun’s effects. Satellites are vulnerable to the shower of energetic particles from the sun, which can damage computer chips and lead to charge build up that affects the electronics within. Periods of intense solar activity can heavily perturb the earth’s magnetic field, causing geomagnetic storms. These geomagnetic storms can cause variations in the Ionosphere, a charged layer of our atmosphere, that can negatively effect radio communication and GPS. Astronauts beyond the protection of the earth’s magnetic field exposed to solar energetic particles produced during solar flares would receive large doses of radiation, equivalent to hundreds of dental x-rays, that can lead to radiation poisoning (Temmer, 2021, and references therein) As our technology advances, and our society becomes less confined to the surface of the earth, it is

becoming increasingly important that we improve our understanding of, and our ability to predict, the activity of our closest star.

Where does the sun's energy and magnetic field come from?

Energy produced in the sun originates from nuclear fusion in the core, where temperatures reach approximately 15 million kelvin (K). From there energy moves outward through the solar interior until reaching the solar surface which has an average temperature of approximately 6600 K (Priest, 2020). The solar interior consists of three layers: the core, the radiation zone, and the convection zone (Figure 1.1). The *radiation* and *convection* zones are each named after their dominant mode of energy transfer. The transition between the two zones, referred to as the tachocline, is where temperature gradient becomes steep enough that the solar plasma becomes unstable to convection, and is likely where the solar magnetic field originates (Priest, 2020). At the solar surface, and within the convection zone, the sun undergoes differential rotation, with plasma rotating more quickly near the equator than the poles. It is the combination of convective motions, and differential rotation, that are understood to generate the sun's global magnetic field (Judge, 2020; Parker, 1979; Priest, 2014). Magnetic field lines produced in the convection zone rise through the solar surface, up into the solar atmosphere, where they become the dominant player and contribute to a host of spectacular solar events, including those studied in this thesis.

The Solar Atmosphere

The solar surface, referred to as the photosphere, is the base of the solar atmosphere and is defined as the point where photons can escape into space without being reabsorbed by surrounding plasma (Priest, 2014). It is important to note that the photosphere isn't really a surface, but a thin region of plasma with steadily decreasing density and temperature.

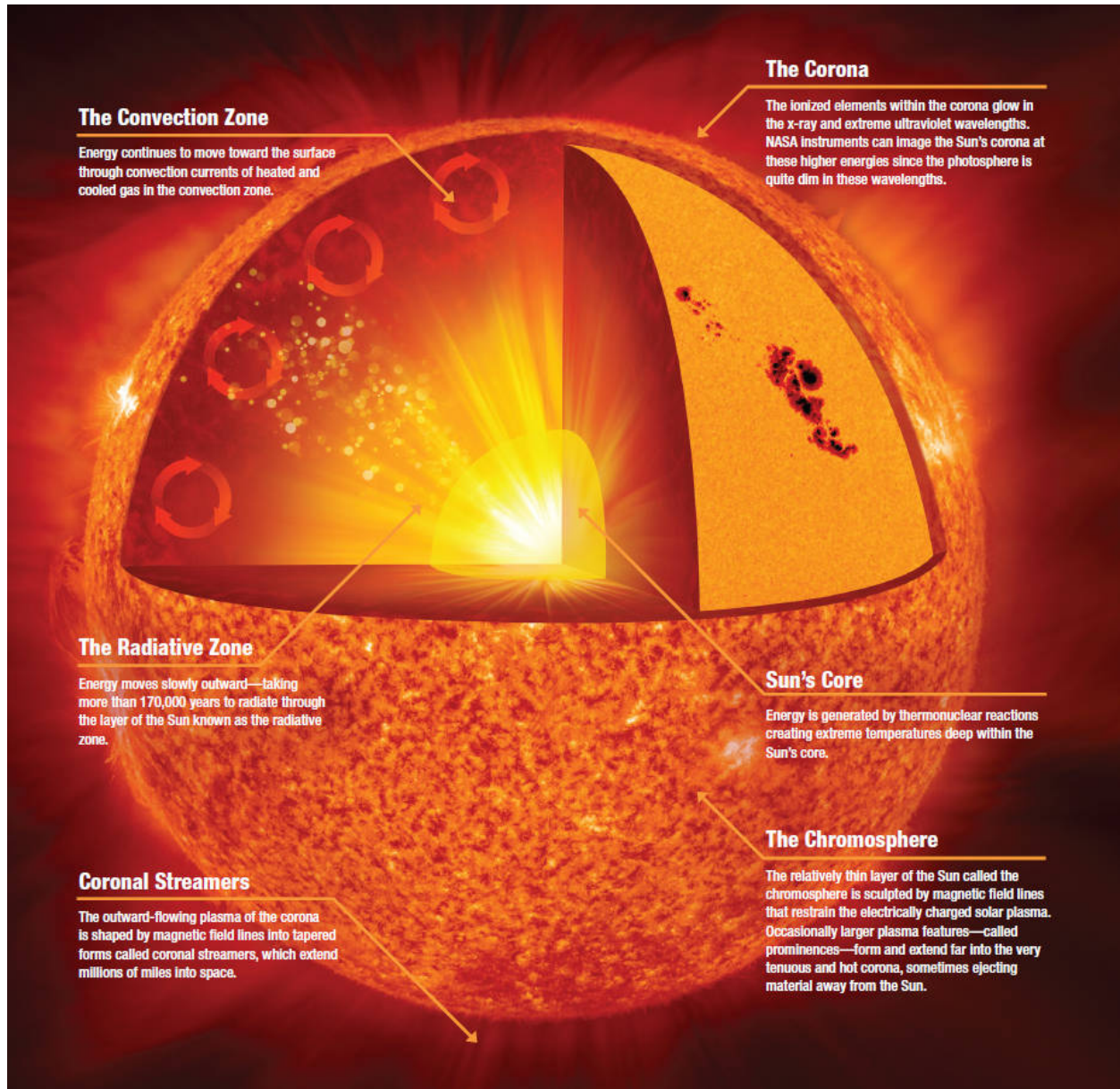


Figure 1.1: The anatomy of the sun from core to corona. Credit: NASA, Mysteries of the Sun

The height of the photosphere is very thin in comparison to the solar radius, ≈ 300 km compared to the $\approx 700,000$ km solar radius, and therefore looks very crisp when observed from earth (Judge, 2020). It is at the edge of the photosphere where the sun reaches an average temperature minimum of ≈ 4400 K (Priest, 2020). The rest of the solar atmosphere consists of (in order of increasing radius) the chromosphere, transition region, and corona (Figure 1.1). The chromosphere, named for the red light it produces that is visible with the naked eye during total solar eclipses, extends approximately 1500 km in height (Priest, 2020). Within the chromosphere the average temperature rises from the temperature minimum to approximately 10,000 K. At the edge of the chromosphere the average temperature increases rapidly to average temperature of approximately 1 million K in the outer most layer of the atmosphere, called the corona (Priest, 2020). The thin region, less than 100 km thick (Priest, 2014), where this transition occurs is appropriately named the transition region.

While it is easiest to think of the solar atmosphere as occurring in one dimensional static layers, in reality it is very structured and dynamic. Above the photosphere, the magnetic field generated in the convection zone expands into a vast canopy of closed loops, with their ends anchored down in the photosphere, as well as open field lines extending out into space. Hotter plasma traces these field lines, allowing us to visualize the complex magnetic field. These magnetic structures have been assigned a whole zoo's worth of names by solar physicists, and are subject to continuous study and debate. Regardless their presence and evolution in images of the solar atmosphere indicate the dynamic and three dimensional nature of the solar atmosphere and make it a very rich area of study.

What are we looking for when we study the solar atmosphere and why?

The solar atmosphere is very hot and violent. As is described above, the solar atmosphere is hotter than the solar surface! Since the roughly 6000 K photosphere does not have sufficient thermal energy to heat the corona to a million degrees, the energy has to

come from somewhere else. A likely source of this energy is the sun's magnetic field (Priest, 2014). The solar plasma, being an almost perfect conductor, is frozen into the magnetic field (Priest, 2014). Therefore, depending on the local plasma conditions, the magnetic field is either drug around by fluid motions, or the plasma is moved by motions in the magnetic field. Beyond the surface of the sun the solar plasma transitions from being fluid dominated, to magnetically dominated. Whether a plasma is fluid or magnetically dominated depends on the ratio of its fluid pressure, p , to its magnetic pressure, p_{mag} , or plasma beta, where,

$$\beta = \frac{p}{p_{\text{mag}}} = \frac{n k_B T}{B^2 / 2\mu_0}, \quad (1.1)$$

and n is the plasma density, T its temperature, and B the magnetic field strength. A plasma with $\beta > 1$ can be manipulated by fluid motion, as is the case in the photosphere and below. As plasma density decreases in the chromosphere and beyond, areas with strong magnetic field strength have $\beta < 1$. In this portion of the atmosphere the magnetic field dominates and magnetic field motions begin to dictate plasma motion (Priest, 2014).

In the solar atmosphere, the magnetic field is complicated and continuously evolving. Fluid motions in the photosphere, driven by the convection and differential rotation, shuffle the base of magnetic loops and open filed lines, known as foot points, changing the field above. Also, new magnetic field lines are constantly being brought to the surface, a process called flux emergence, that interact with the field above. As the magnetic field is shuffled around, and interacts with emerging flux, it is twisted and tangled gaining energy, until, somewhat suddenly instability sets in. These instabilities allow the magnetic field lines to reconfigure themselves into a lower energy state, a process referred to as magnetic reconnection (Parker, 1957; Petschek, 1964). When field lines reconnect, energy stored in the magnetic field is quickly converted to kinetic energy, and plasma is accelerated to velocities much greater than would be possible through thermal means. The velocity at which waves travel along

magnetic field lines, which occurs post reconnection, is known as the Alfvén speed. In areas of strong magnetic field the Alfvén velocity can be an order of magnitude faster than the local sound speed in the plasma (Priest, 2014), which is the fastest speed a wave can travel via fluid processes. Observations of velocities much greater than the sound speed during solar eruptions indicate the important roll of the magnetic field and magnetic reconnection. Also, the correlation between areas of strong magnetic field and eruptive activity, with the hotter parts of the corona, make the solar magnetic field a strong candidate for the excess temperature of the solar atmosphere.

How do we study the solar atmosphere?

Much of what we know about the sun comes from examining the light it produces. We collect light from the sun using a variety of techniques, and from it can determine things like plasma temperature, density, velocity, and elemental content, as well as the magnetic field strength. All of this information can then be pieced together to form a more complete picture of solar events so that we can better inform and test our models and understanding.

The solar atmosphere, being a plasma, consists of charged particles including free electrons and ions. As electrons and ions interact and collide, they experience changes in kinetic energy. These collisions conserve energy, so any energy not stored in the kinetic energy of the particles is either stored, by exciting bound electrons to higher energy states, or released in the form of radiation. Energy is radiated away as a photon, a discrete packet of light, with a specific wavelength, λ , where the energy,

$$E = \frac{hc}{\lambda}, \quad (1.2)$$

h is Plank's constant, and c is the speed of light. Therefore, by measuring the wavelength of a photon, we know its energy. Energy stored in an ion's bound electron is also eventually

emitted as a photon when the bound electron transitions from an excited state, to a more stable one. Since these transitions occur in distinct steps, the wavelength of a measured photon can also tell us what kind of ion produced it. Since ions in the solar plasma are often moving, either because of thermal motions or changes in the magnetic field, the wavelength of emitted photons are often Doppler shifted. Just as train whistle sounds higher or lower pitched depending on if the train is moving toward or away from you, emitted photons have shorter or longer wavelengths depending on the ions velocity. Slight deviations from a photons expected wavelength tell us the ion's velocity,

$$v = c \frac{\lambda - \lambda_0}{\lambda_0}, \quad (1.3)$$

where λ is the measured wavelength and λ_0 is the emitted wavelength at zero velocity. Photons of shorter wavelength are referred to as blue shifted, an analogy to visible light, and longer wavelengths red shifted. In solar physics the convention is to define the positive direction as away from us and toward the sun, therefore blue shifted photons have negative velocity and are traveling toward us, and red the opposite.

Radiation emitted from the sun, referred to as the solar spectrum, spans a massive range of wavelengths from gamma rays (picometers) to radio waves, with it's peak emission being visible light ($\approx 400 - 700$ nm) (Judge, 2020). While the solar spectrum is broadly peaked around visible light, zooming in reveals many smaller peaks and dips at various wavelengths (Figure 1.2). These peaks and dips are from ions emitting or absorbing photons at specific wavelengths, referred to as spectral lines, are the key to isolating and studying different portions of the solar atmosphere. Using filters we can isolate and image narrow wavelength ranges. Images of the photosphere can be captured from earth, since visible light easily passes through the Earth's atmosphere. In order to image the rest of the solar atmosphere, we image the sun in shorter wavelengths, in which the photosphere is very

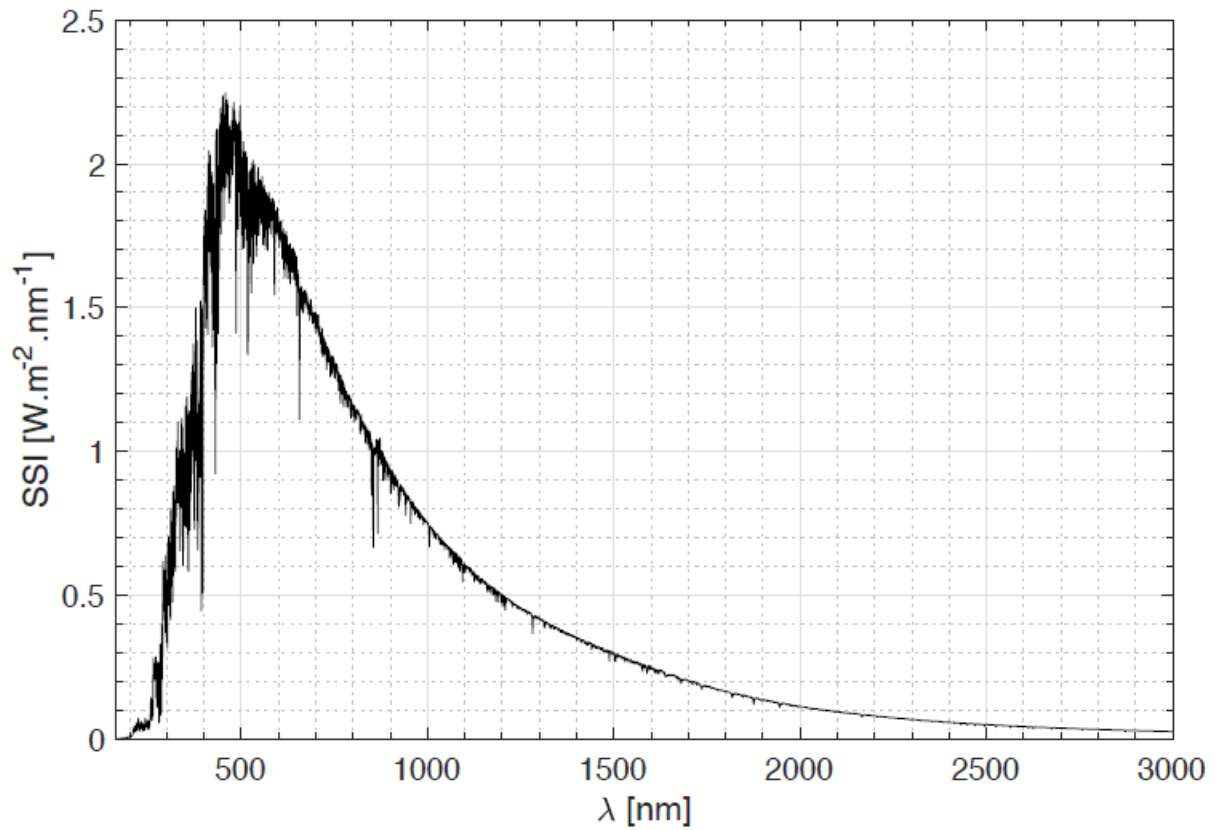


Figure 1.2: The solar spectrum captured in April 2008 by the Solar instrument onboard the International Space Station. ©CNRS

dim. Also, spectral lines in the ultraviolet and shorter wavelengths tend to be optically thin, meaning emitted photons aren't readily absorbed by adjacent ions once emitted. This allows us to image deeper layers in the solar atmosphere.

Shorter wavelengths, from ultraviolet to x-ray, are readily absorbed by the Earth's atmosphere, and therefore must be imaged from space. The currently operating Atmospheric Imaging Assembly (AIA: Lemen et al., 2012) on board the Solar Dynamics Observatory (a satellite with multiple solar instruments), uses narrow filters to image the sun in several different Extreme Ultraviolet (EUV) wavelength ranges aimed at isolating bright spectral lines emitted by the solar atmosphere. Figure 1.3 shows four of these images centered around 304 Å, 171 Å, 193 Å, and 335 Å wavelengths. From quantum mechanics we know the dominant spectral lines come from He II, Fe IX, Fe XII, and Fe XVII ions that occur most often at 0.05 MK, 0.63 MK, 1.2 MK, and 2.5 MK respectively. These filtered images allow us to image the solar atmosphere at various heights and temperatures so we can better understand the structure of solar features and events. Unfortunately most filters aren't narrow enough to truly isolate individual spectral lines or portions of them. Therefore in order to increase our spectral resolution we use a different instrument, the spectrograph.

The spectrograph is a fundamental tool for better understanding light coming from the sun. Spectrographs use diffraction gratings to disperse light based on its wavelength, allowing you to examine the spectral content. Typically light traveling through a spectrograph will be focused through a slit, a very narrow strip for light to travel through, prior to being dispersed by a diffraction grating. These are referred to as slit spectrographs. When used to image the sun, this results in an image of practically pure spectral signal over taken from a very narrow strip of sun in the direction perpendicular to the slit. The Interface Region Imaging Spectrograph (IRIS: De Pontieu et al., 2014) is a currently operating satellite based slit spectrograph imaging the sun. Slit spectrographs like IRIS build spectrally resolved images, an image of the sun with spectral information at every pixel, by scanning the slit over a

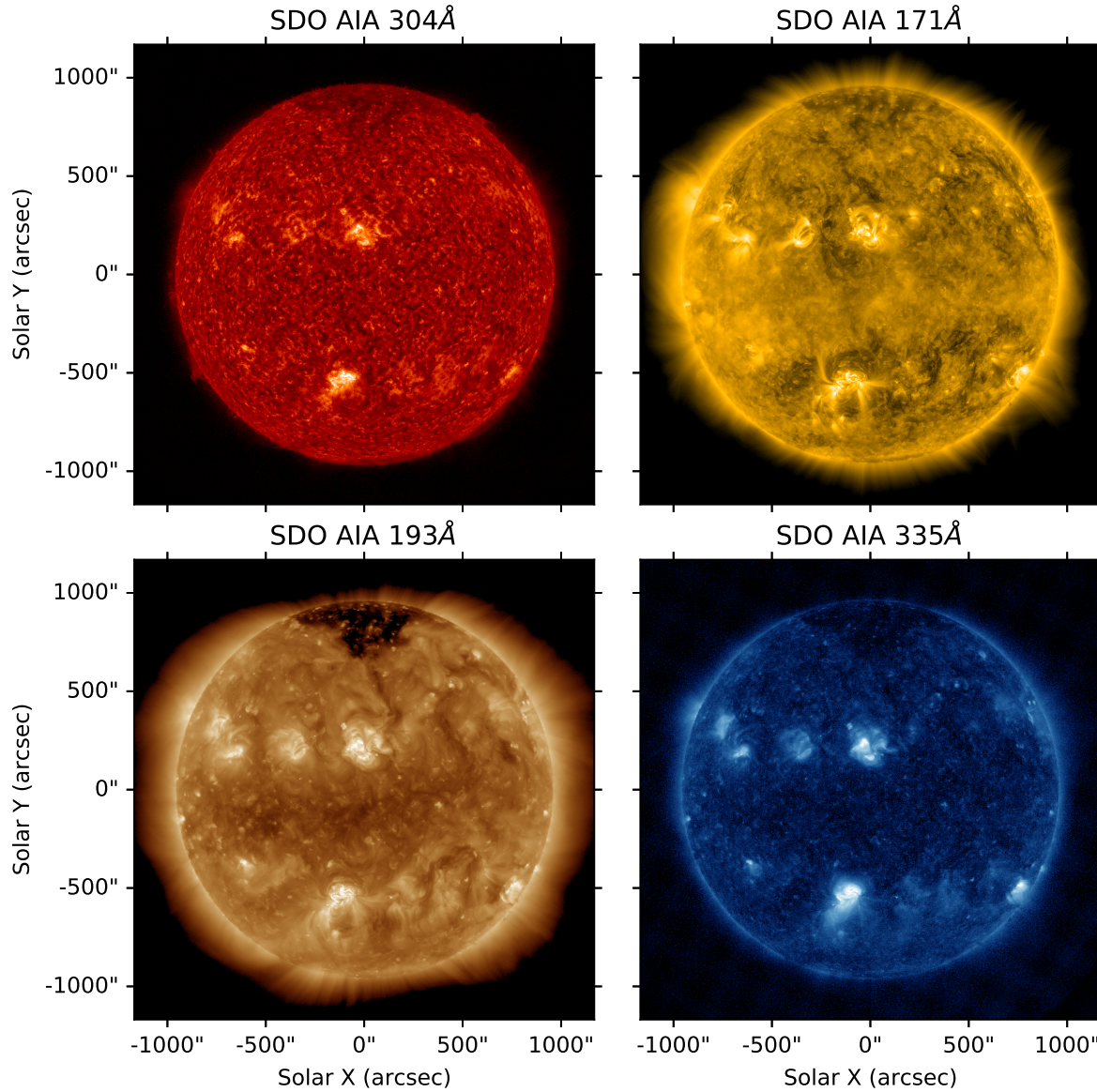


Figure 1.3: Extreme Ultraviolet images from four different AIA channels. Narrowband images of the sun allow us to study different layers of the solar atmosphere by isolating wavelengths from emission lines known to form most often at specific temperatures. These images are displayed in log scale to increase contrast and the color tables are synthetic (since these are not visible light images) and assigned by the instrument team.

wider field of view, referred to as rastering. Images from a rastered slit spectrograph can achieve very high spatial and spectral resolution over a decent size field of few. For example, a large IRIS raster has a .33 arcsecond spatial resolution and $\approx 3 \text{ km s}^{-1}$ per pixel spectral resolution over a $\approx 2 \times 3$ arcminute field of view (De Pontieu et al., 2021). The down side of rastering a slit spectrograph is that a full exposure is required at every position, which with the current sensitivity of IRIS, takes ≈ 10 s per exposure. This results in a spectrally resolved image taken over the course of ≈ 50 minutes for a 320-step raster. For more static solar scenes, with less activity, this trade off can have little effect. Unfortunately, many solar eruptions evolve on second timescales, causing the scene to constantly change as you try to image it, often resulting in the slit being pointed away from an area of interest.

An alternate approach is to remove the slit, and disperse an image over a much larger field of view using a diffraction grating, often referred to as a slitless spectrograph. Images from a slitless spectrograph have overlapping spatial and spectral information in every pixel. Therefore, in order to capture a spectrally resolved image of the sun, images from multiple slitless spectrograph channels need to be combined and ‘inverted’ (e.g. Kak & Slaney, 2001). These instruments, referred to as Computed Tomography Imaging Spectrographs (CTIS: Descour & Dereniak, 1995), use the same principle as a CT (Computed Tomography) scan in a doctors office that combine a series of unique two dimensional images taken from different angles, to form something three dimensional. The primary difference between a CTIS instrument and a CT scan is that the goal of a CT scan is the capture a data cube with three spatial dimensions, $I(x, y, z)$, whereas a CTIS instrument returns a cube with two spatial dimensions and one spectral dimensions, $I(x, y, \lambda)$. Compared to slit spectrographs, CTIS instruments can capture spectrally resolved images over wide fields of view at much a much faster cadence, but introduce spatial-spectral ambiguity in each image which can be difficult to disentangle. The Multi-Order Solar Extreme Ultraviolet Spectrograph (MOSES: Fox et al., 2010) and Extreme ultraviolet Snapshot Imaging Spectrograph(ESIS: Smart et al.,

2021), are two CTIS instruments developed at Montana State University. Data from both instruments are used in this thesis.

Thesis Outline

The content of this thesis is divided into three chapters. While the projects described in each chapter are unique, they all share a common thread, the transition region. The transition region is a fascinating area of solar study for a couple reasons. First, all mass and energy moving between the chromosphere and corona travels through the transition region. By tracking mass and energy flux between the upper and lower solar atmosphere we can better track how the corona is heated and observe the types features and events associated with that heating. Second, the transition region is where the solar atmosphere becomes magnetically dominated and is littered with magnetically driven phenomena. Eruptions of the transition region are often much smaller than the large flares of the corona, which makes them more difficult to spatially resolve, but they are also more frequent, making it easier to capture them with limited field of view instruments, and build statistics on their nature. Also, since these events occur more frequently, it is much easier to capture them with a sounding rocket based instrument that only has five minutes to image the sun. The transition region is also very thin, making it easier to pinpoint the location of photon emission and form a clearer picture of the geometry of a spatially resolved event. The primary instruments used in the following studies (IRIS, MOSES, and ESIS) all aim measure intensity and velocity at various heights in the transition region. The following chapters describe unique measurements of the transition region and discuss their possible implications on our understanding of the sun.

The first chapter develops a model of magnetic reconnection used to describe the observation of elliptical motion in a flare ribbon observed by Brannon et al. (2015). On April 18, 2014 IRIS observed an M-class flare with a sit-and-stare that captured one of two flare ribbons. Brannon et al. (2015) observed a sawtooth pattern that propagated along the

ribbon with a phase velocity of $\approx 15 \text{ km s}^{-1}$. This motion resulted in oscillations in both velocity ($\pm 20 \text{ km s}^{-1}$) and intensity along the slit ($\pm .5 \text{ arcseconds}$) that were 180 degrees out of phase. Using a model of the Tearing Mode instability (Furth et al., 1963) occurring in a reconnecting current sheet across which there is also velocity shear, we were able to reproduce the oscillations in velocity and intensity, as well as the phase velocity of the wave. We also propose a magnetic geometry and local plasma conditions for the flare that support this hypothesis.

The second chapter describes a method used to quantify the total spectral content in images from the first flight of MOSES. Early work on MOSES data revealed solar features that could not be attributed to the principal wavelength in the passband, He II 304 Å, or other obvious sources of contamination. We also found signatures of this contamination in the mean cross-correlation of MOSES difference images. In order to identify and quantify this contamination, we fit synthetic MOSES images with known spectral content to the actual MOSES images. Synthetic MOSES images were formed from images captured by the Extreme-ultraviolet Imaging Telescope (EIT: Delaboudinière et al., 1995) and synthetic spectra from the Chianti database (Del Zanna & Young, 2020; Dere et al., 1997). The best fit synthetic data was found by varying the average Differential Emission Measure (DEM) over the MOSES field of view used to create the synthetic spectra until the difference between the MOSES and synthetic difference image cross-correlation was minimized. We also comment on the elements of the MOSES design that led to this contamination and confusion, and how it might be improved for similar instruments in the future.

The third chapter explores data from the first flight of the ESIS sounding rocket launch. ESIS improves on the design of MOSES by adding an additional channel (with room for up to six in future flights), and an intermediate focal plane with a field stop that more clearly defines its field of view. During its roughly 5 minutes of observing time ESIS captured tens of small solar eruptions, referred to as explosive events (Dere et al., 1989), and one larger jet

($\approx 20'' \times 40''$) over the ≈ 11.5 arcminute field of view. We describe how the unique images were prepared into multiple data levels, and both a qualitative and quantitative approach to understanding the data. Using the dominant spectral line in the ESIS passband, O V 630 Å, we demonstrate how the difference between features in O V captured by different ESIS channels can be used to “read off” qualitative information about an events velocity, and its evolution in time. We also use a Multiplicative Algebraic Construction Technique (MART: Okamoto & Yamaguchi, 1991; Verhoeven, 1993) to combine data from all four ESIS channels and invert two different explosive events and show their evolution.

Finally, following these three chapters, I summarize the discussion and conclusions from each chapter. I also offer some thoughts on the impact of this work, and implications for future studies in solar physics.

REFERENCES CITED

- Brannon, S. R., Longcope, D. W., & Qiu, J. 2015, ApJ, 810, 4
- De Pontieu, B., et al. 2021, Sol. Phys., 296, 84
- De Pontieu, B., et al. 2014, Sol. Phys., 289, 2733
- Del Zanna, G., & Young, P. R. 2020, Atoms, 8, 46
- Delaboudinière, J. P., et al. 1995, Sol. Phys., 162, 291
- Dere, K. P., Bartoe, J. D. F., & Brueckner, G. E. 1989, Sol. Phys., 123, 41
- Dere, K. P., Landi, E., Mason, H. E., Monsignori Fossi, B. C., & Young, P. R. 1997, A&AS, 125, 149
- Descour, M., & Dereniak, E. 1995, Appl. Opt., 34, 4817
- Fox, J. L., Kankelborg, C. C., & Thomas, R. J. 2010, ApJ, 719, 1132
- Furth, H. P., Killeen, J., & Rosenbluth, M. N. 1963, Physics of Fluids, 6, 459
- Judge, P. G. 2020, *The Sun: A Very Short Introduction*
- Kak, A., & Slaney, M. 2001, *Principles of Computerized Tomographic Imaging*, Classics in Applied Mathematics (Society for Industrial and Applied Mathematics)
- Lemen, J. R., et al. 2012, Sol. Phys., 275, 17
- Okamoto, T., & Yamaguchi, I. 1991, Optics Letters, 16, 1277
- Parker, E. N. 1957, J. Geophys. Res., 62, 509
- Parker, E. N. 1979, *Cosmical magnetic fields. Their origin and their activity*
- Petschek, H. E. 1964, Magnetic Field Annihilation, Vol. 50 425
- Priest, E. 2014, Magnetohydrodynamics of the Sun
- Priest, E. 2020, Solar physics: Overview
- Smart, R. T., et al. 2021, In preparation for ApJ
- Temmer, M. 2021, Living Reviews in Solar Physics, 18, 4
- Verhoeven, D. 1993, Appl. Opt., 32, 3736